Uncovering dual pathways for the sense and control of balance through reaction-time analysis

H.J. Steketee

Delft University of Technology

TU Delft

Uncovering dual pathways for the sense and control of balance through reaction-time analysis

by

H.J. Steketee

In partial fulfillment of the requirements for the degree of Master of Science in Biomedical Engineering Medical Devices

at the Delft University of Technology,

to be defended publicly on Friday July 11, 2025 at 9:30 AM.

Supervisor:	Prof. dr. ir. A. C. Schouten,	TU Delft, supervisor
Thesis committee:	Prof. dr. ir. P. A. Forbes,	Erasmus MC
	Dr. D. Dodou,	TU Delft
	L. Mensink,	Erasmus MC

Cover: Robotic balance simulator at the Sensorimotor Neuroscience and Biorobotics lab of the Erasmus MC
Style: TU Delft Report Style

An electronic version of this thesis is available at http://repository.tudelft.nl/.

TU Delft

Summary

Reaction-time paradigms are widely used to investigate multisensory processing and sensorimotor integration, yet their application to postural control has been limited. This may stem from the view that most self-generated balance-correcting motor actions occur without conscious awareness. However, this contrasts with evidence that reaction times to external stimuli can still be modulated during balance tasks (e.g., sitting, standing, walking), suggesting that even automatic balance control can interact with higher-level cognitive processing. Yet the temporal dynamics distinguishing automatic postural from consciously mediated responses to balance perturbations remain underexplored. In this study, we used a robotic balance simulator to impose disruptions to ongoing balance and dissociate balance-correcting and perceptual mechanisms of standing balance control. Participants stood on a robotic simulator that applied 200 ms torque perturbations of varying amplitudes. Additional ankle torque perturbations mimicking natural balance-control statistics were delivered to artificially increase ongoing motor noise. We recorded both EMG-based corrective muscle responses and perceptual reaction times via button presses, enabling direct comparison of automatic and conscious responses. Both response types decreased with increasing perturbation amplitude, consistent with findings from other sensory domains. Crucially, perceptual reaction times increased with higher noise amplitudes, whereas automatic postural responses did not. This dissociation highlights distinct neural mechanisms underlying conscious perception and postural control based on the functional purposes these processes fulfill.

Contents

1

Introduction

Human standing balance control relies on the nervous system's ability to accurately sense our motion and orientation in space. To achieve this, the nervous system maintains an internal model of the body, constructed through the integration of signals from the visual, vestibular, somatosensory, and auditory systems. Based on this internal representation, the balance controller within our nervous system actively regulates motor commands to stabilize the body via subcortical pathways. Because most balance regulation occurs unconsciously, consciously detecting the current state of balance happens primarily when postural stability is challenged, even though it is sensed continuously by the nervous system.

It had long been assumed that the nervous system maintains a single representation of the body, which is used for both the subconscious control of balance and the conscious detection of balance disturbances (Gurfinkel et al. 1988; Massion 1994; Kandel et al. 2021). However, recent research has challenged this notion, showing inconsistencies between the actions resulting from automatic postural control and the conscious perception of balance. For instance, postural responses can be generated outside of conscious awareness (Jacobs and Horak 2007; B. Luu 2010). When perturbation velocities fall within the natural range of variability of quiet standing, the balance controller can sense, integrate, and respond to the perturbation in the absence of conscious detection, resulting in the postural response being detected as the external disruption (Tisserand et al. 2022). Moreover, when balance control is subtly taken over by computer control, vestibular-evoked balance responses can be disengaged before the transition to computer control is consciously detected (B. L. Luu et al. 2012). The balance controller also responds to increases in ankle torque noise at noise magnitudes below the perceptual threshold (Mensink et al. 2025). These findings suggest that the detection and control of balance do not share a single representation of the body and may utilize sensory information according to separate mechanisms.

To reveal the disparity between the sensing of balance information for postural control and conscious detection of balance, previous work has utilized psychophysical threshold detection paradigms, to determine the minimum intensity of a stimulus that participants can reliably detect is (Mensink et al. 2025). However, this approach simplifies detection to a binary choice, thereby failing to capture the dynamic processes involved in detecting and responding to external stimuli. In contrast, reaction time (RT) paradigms do capture these dynamics in differences in detection delay between stimuli (Donders 1969). RT studies on the visual, auditory, and somatosensory domains model for decision-making (Posner 1980; Mansfield 1973; Palmer, Huk, and Shadlen 2005; Veugen, Opstal, and Wanrooij 2022; Prinzmetal, McCool, and Park 2005; Noorani and R. H. Carpenter 2016). According to the model, the detection system maintains a decision signal that rises linearly based on sensory input, accumulating evidence until it reaches a set decision threshold, at which point the stimulus is detected. Stronger stimuli generate faster-rising decision signals, resulting in faster reaction times. A normally distributed variability in this rate of evidence accumulation would result in the signature distribution of RTs that is skewed towards faster responses. Despite their value in uncovering how stimulus properties influence perception, RT approaches remain underused in balance research. A single study found that reaction times decreased as the amplitude of support surface perturbations increased, according to the model

described by Noorani and Carpenter (2016) (Richerson et al. 2004). However, the onset of muscle activation during postural responses appears invariant to perturbation amplitude, with only response magnitude scaling with increased perturbation amplitude (Diener, Horak, and Nashner 1988; Horak, Diener, and Nashner 1989). This suggests that automatic postural control employs a different mechanism for sensory integration than the conscious detection of balance. However, the mechanisms driving the conscious detection of disturbances and balance responses have not been investigated simultaneously.

The processes involved in perceiving and correcting for external balance perturbations can be influenced by uncertainty arising from both motor and sensory sources. This uncertainty is introduced by noise generated during the sensory encoding of body motion, in central processing, and through active force production. This uncertainty in the balance control loop can distort our internal model (Wolpert, Ghahramani, and Jordan 1995), and noise from active force generation can lead to a mismatch between intended and actual body acceleration (Kiemel, Oie, and Jeka 2002). Motor noise can be experimentally manipulated using a robotic balance simulator by modelling ankle torque noise based on the magnitude and dynamics of each participant's torque profile (Mensink et al. 2025). This approach has demonstrated that the nervous system accommodates for motor noise through subconscious adaptations, such as modulating vestibulomotor gain. While this study identified the perceptual threshold for increased motor noise, it remains unclear whether, and to what extent, motor noise can influence the detection or the postural responses to balance perturbations.

In this study, the mechanisms that drive conscious detection and automatic postural control were investigated. Using a robotic balance controller, ankle torque perturbations that mimic both externally imposed disturbances and natural ankle torque noise were presented. Conscious detection of balance disturbances was analyzed through RTs measured via button presses, while the detection relied on by the balance controller was assessed from the onset of postural balance responses. This revealed that both processes operate according to the same detection mechanisms where response time decreases with increasing perturbation amplitude. Furthermore , by simultaneously presenting the two perturbation types, the sensitivity to ankle torque noise of both the conscious perception and automatic postural responses is examined. The signal-to-noise ratio is shown to only affect the conscious detection of balance disturbances, while the timing of postural response is insensitive to ankle torque noise.

2

Methods

2.1. Participants

A total of 8 healthy adults (4 females, age: $\mu \pm \sigma = 28 \pm 6.9$ years; range 22-45 years) with no history of balance, neurological, or musculoskeletal disorders volunteered to participate in this experiment. The experimental protocol was verbally explained before the experiment , and written informed consent was obtained. The experiment was approved by the Medical Research Ethics Committee Erasmus Medical Center and conformed to the Declaration of Helsinki.

2.2. Experimental set-up

Participants stood on a robotic balance simulator that simulates natural human standing balance in the anteroposterior (AP) and mediolateral (ML) planes (Fig. 1A). Participants were secured to the robot using seatbelts attached to the torso and hip harnesses, which were connected to a rigid backboard. The backboard and torso/hip harnesses can move in the anterior-posterior (AP) and mediolateral (ML) directions, respectively. Participants controlled their motion through ground reaction forces and torques exerted on the force plate (AMTI BP400 × 600; Watertown, MA, USA). The mechanical load of the body was simulated as an inverted pendulum by a real-time motion controller (PXI-8880; National Instruments, TX, USA) running at 500 Hz. While standing in the robotic balance simulator, the motor actions generated by the participants were converted by the robotic system to the angular position, velocity, and acceleration of their center of mass (CoM). The transfer function relating the changes in ankle torque to kinematics is described in (Qiao et al. 2023). The AP CoM angle is directly related to the movement of the backboard, while the ML CoM angle is decomposed into linear movements of the pelvis and torso at the harnesses (Qiao et al. 2023). The entire system operated with a delay of 6- 10 ms between position commands sent to the robot and changes in the backboard angle or harness position. Additional details on the robot's setup and design can be found in (Rasman, Forbes, et al. 2018). Angular whole-body movement limits were set between 6˚ anterior and 3˚ posterior, and between ± 4˚ mediolaterally, as determined by software limits. Angular whole-body movement was restricted to ensure that participants could generate sufficient torque to move out of the limits if they were exceeded while balancing across the range of normal quiet standing (Forbes et al. 2016; Rasman, Blouin, et al. 2024).

Whole-body movement was simulated using an inverted pendulum model (Fig. 1B), which treated the body as a concentrated-mass system. Participant parameters included in the simulation were: mass ($\mu \pm \sigma = 68.9 \pm 14.6$ kg), height ($\mu \pm \sigma = 177 \pm 12$cm), CoM height ($\mu \pm \sigma = 88 \pm 5$cm), ankle height ($\mu \pm \sigma = 8.4 \pm 0.9$ cm), and stance width ($\mu \pm \sigma = 17 \pm 1.2$ cm). CoM height was determined by having participants lie on a rigid board balanced over a round rod oriented orthogonally to the body. The board was rolled longitudinally over the rod until the participants' mass was balanced. The CoM height was measured as the distance between the ankle joint and the tipping point of the board. Ankle height was estimated as the height from the floor to the mean of the right medial and lateral malleoli. Stance width was set equal to measured hip width.

To measure the postural balance response generated by automatic postural control , surface EMGs were collected . Data were collected from three muscles of the right lower leg: the tibialis anterior (TA), medial gastrocnemius (mGAS), and the soleus (SOL) muscles. These muscles were selected as they are major contributors to the postural responses to anterior perturbations. This involves the contraction of the plantarflexor muscles, such as the SOL and mGAS, and the inhibition of the TA, a dorsiflexor muscle (Campbell, Dakin, and M. G. Carpenter 2009). To obtain EMG signals, self-adhesive AG-AgCl surface electrodes (Blue Sensor M, Ambu A/S, Ballerup, Denmark) were used with an inter-electrode distance of 2 cm. Electrodes were placed according to the anatomical landmarks described by (Perotto and Delagi 2005). The skin was prepared by cleaning with isopropyl alcohol and scrubbing with skin preparation gel (Nu-Prep, Weaver and Company, Aurora, CO, USA). For data analysis, only the mGAS was used as it provided the most robust response.

2.3. Protocol

2.3.1. General procedure and familiarization

Prior to each experiment, participants familiarized themselves with the control of the robotic balance simulator. Participants were informed that balancing in the robot resembles natural standing. Upright balance in the AP direction was maintained by producing dorsiflexion and plantarflexion torques around the ankles. Upright balance in the ML direction was maintained by generating torques around the ankle as well as by modulating the vertical forces between each foot. Participants were also instructed to move into the AP and ML limits to understand the extremes of their balancing movement in the robot and to ensure they could get out of the limits during the experiment. In doing so, participants were aware that the robotic simulator would safely prevent them from falling.

During the experiment, participants wore a blindfold and noise-cancelling headphones playing white noise to exclude balance-related visual and auditory input. Participants could reacquaint themselves with controlling the robotic balance simulator under these conditions. Participants were presented with three types of perturbations conducted over two sessions on separate days. The first session consisted of a baseline measurement followed by two types of perturbations, the pulse-only and noise-only conditions. Perturbations in the pulse-only condition consisted of 200 ms pulses of varying amplitudes (2, 4, 8, and 16 deg/s^2), and the noise-only condition perturbations mimicked natural balance-control ankle torque statistics (0, 0.4, 0.8, 1.2, and 1.6 times standard deviation (SD)). The order of pulse-only and noise-only conditions was randomized between participants. In the second session, participants were subjected to the pulse-in-noise condition, consisting of trials where the pulse-only and noise-only perturbations were added together.

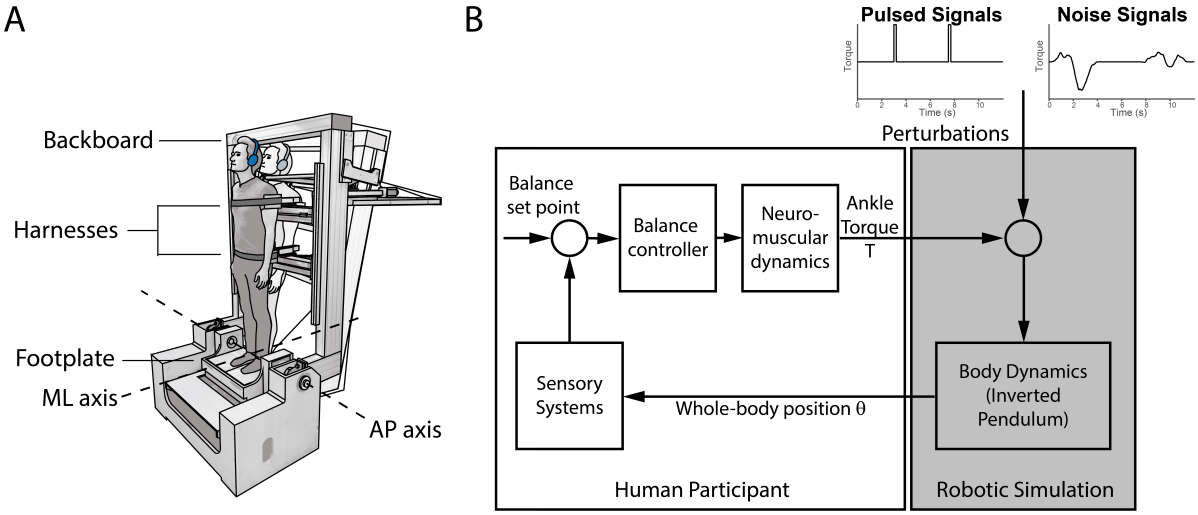

Figure 1. Experimental design and block diagram of robotic balance simulation. (**A**) The participant stood on a force plate and was secured to the backboard at the shoulder and hip harnesses. The backboard is controlled by a motor, enabling it to move in the anterior-posterior plane. The hip and shoulder harnesses are independently controlled by two motors that move the participant in the mediolateral plane. The motion of the backboard, as well as the hip and shoulder harnesses, was based on the mechanics of an inverted pendulum model, taking the forces exerted on the force plate as input. The backboard moved around the anterior-posterior (AP) axis that passed through the participant's ankles. Forces exerted around the mediolateral (ML) axis, between the center of the feet, are converted to movement of the harnesses. (**B**) Control loop of the human participant and robotic simulator used to mimic and manipulate standing balance. The desired balance set point is internally compared by the nervous system with the current position as sensed by the sensory system. The balance controller uses this difference to initiate motor commands to achieve the desired position. The resulting ankle torque (T) is exerted on the footplate and registered by the robotic simulation. Here, an additional torque signal can be added. The sum torque signal is converted to a whole-body position (θ) according to an inverted pendulum model. The participant is then moved to this resulting whole-body position. During the experiments, a torque signal consisting of pulses, noise, or a combination of the two was added to the participant-generated torque signals.

2.3.2. Pulse-only

To determine response times to defined balance perturbations, in the pulse-only condition, participants were exposed to trials of 200 ms pulsed torque perturbations that imposed whole-body accelerations in the anterior direction. Four pulse amplitudes were presented, corresponding to accelerations (α) of 2, 4, 8, and 16 deg/s^2. These accelerations were converted to torque magnitudes (τ) using participants' mass (M), height (H), ankle height (ankH), and the inertia factor of the system (I) according to the following equation:

$$\tau = \alpha_{radians} MI(H - ankH) \qquad (Eq.1)$$

Participants were instructed to press the button when they detected sudden balance perturbations. Trials were presented with a randomized uniform interstimulus interval ranging from 3250 to 5000 ms in 250 ms increments. Each pulse level was presented 25 times, resulting in a total of 100 trials. The condition took approximately 10 minutes to complete.

2.3.3. Noise-only

Response times to ankle torque noise were investigated in the noise-only condition. In the noise-only condition, trials consisted of an 8 s periods during which additional ankle torque noise was applied, resulting in both anterior and posterior body motion. The torque noise was generated by filtering white noise according to the dynamics of each participant's ankle torque profile from the baseline measurement. The filtered signal was smoothed over a 1-second period on both ends by multiplying by a normalized raised-cosine, between 0 and 1 for the onset and 1 to 0 for the tail. Then the resulting signal scaled to match each participant's baseline variability (SD). Five levels of ankle torque noise were presented, created by multiplying the noise signal by 0, 0.4, 0.8, 1.2, or 1.6. Trials with no added noise perturbation (i.e., scaling SD = 0) were included to assess the false-positive response rate. Participants were instructed that the balance perturbations were more gradual and to press the button whenever

they perceived any disturbance to their balance. The interstimulus interval was uniformly randomized between 520 ms and 6000 ms in 250 ms increments. Each noise level was presented 25 times, resulting in a total of 125 trials. The condition took approximately 30 minutes to complete and was split up into two 15- minute segments with a break in between to prevent fatigue.

2.3.4. Pulse-in-noise

In the combined experiment, the pulse and noise perturbations were presented together. Participants were instructed to press when they perceived sudden balance disturbances (i.e. pulse perturbations). Combinations of two pulse amplitudes (4 and 8 deg/s^2) and all noise levels were made. The noise signal was generated for a 4 s period. The pulse was presented at either 0, 1, 2, or 3 s after the onset of the noise. Note that we only report on conditions 0 and 3 s lead time here. These amplitude levels and delay times were based on findings from pilot studies and chosen to offer tasks of sufficient difficulty in terms of pulse amplitude and span the time needed to respond to noise stimuli. Pilot studies showed pulse amplitudes of 4 and 8 deg/s^2 were almost always detected but RTs for the 4 deg/s^2 were slower than those for 8 deg/s^2. Mean detection of noise stimuli was between 1 and 4 seconds for the different noise levels, which is covered by the chosen lead times. The interstimulus interval must be uniformly distributed to ensure that detection of pulses presented earlier or later than the average (1.5 s) is not influenced by the unconscious prediction of pulse timing based on the stimulus distribution. To achieve this, noise periods were preceded by a compensatory delay based on the lead time of the trial, resulting in the pulse being presented uniformly between 3500 and 4250 ms in 250 ms steps after the end of the previous noise period. This set consisted of 40 conditions (two pulse amplitudes, five noise levels, and four leading times), each presented 25 times, resulting in 1000 trials. To prevent fatigue, a 5-10 min break from standing was provided after 80 trials, where participants could sit or walk around. Excluding breaks, the experiment took 100 minutes in total.

2.4. Data acquisition and analysis

Signals for the real-time control of the robotic simulation were processed by an FGPA module (PXI-7846R; National Instruments, Austin TX, USA) and sampled at 500 Hz. A Refa 128-channel stationary amplifier system sampled the EMG data at 2048 Hz (REFA amplifier, TMSi, Oldenzaal, the Netherlands). All data was processed in MATLAB software (2023b version, Mathworks, Natick, MA, USA) and the EEGLAB toolbox (2022.0 version (Delorme and Makeig 2004)) was used to process EMG data. Statistical analysis was also performed in MATLAB, with an alpha significance of 0.05.

2.4.1. Reaction times

RTs were extracted from participants' button presses as the time between perturbation onset and the first button press following the perturbation . Note that RT distributions are typically right skewed and cannot easily be described with simple statistical parameters like mean and standard deviation (Ulrich and Miller 1994; Ratcliff 1993; Whelan 2008). To normalize RT distributions, RT data were transformed to their reciprocal (1/reaction time), into promptness, with unit 1/s (Ratcliff 1993; R. H. S. Carpenter and Williams 1995).

Before obtaining the mean and standard deviation of the promptness distribution, the RT data were visualized using dot raster and reciprobit plots to identify outliers, participant performance , and infer normality of promptness distributions. Reciprobit plots were created by first transforming the promptness distribution to a function of the cumulative probability over time (Noorani and R. H. Carpenter 2016). Next, a line is fitted to the data within the 25th and 75th percentiles of the resulting distribution. Using the 25th and 75th percentiles captures the main trends in the data while reducing the influence of outliers, which ensures a more robust fit. Normally distributed promptness data aligns with the straight-line fit performed for the recipobit plots, as the data is plotted on a non-linear probit scale (Noorani and R. H. Carpenter 2016)). Based on visual inspection, RT thresholds were defined for excluding outliers in the data. For the pulse-only condition, RTs < 150 ms were excluded, and for the noise-only, RT < 500 were excluded. The exclusion criterion for the combined experiment was set equal to that determined for the pulse-only condition, as the same stimulus was the target of detection in both conditions.

After removing the outliers from the distribution, the mean (μ_P) and standard deviation (σ_P) of the remaining promptness distributions are calculated. For easier interpretability, mean promptness was then

transformed back to RT ($\mu_{RT} = 1/\mu_P$) by taking its reciprocal. Note, however, that this approach may lead to underestimated mean reaction times estimated directly from the data (Jensen 1906)). However, if the promptness distribution is approximately normal with low variance, the error introduced by this approximation is negligible. Standard deviation of promptness was converted to the standard deviation of RT (σ_{RT}) as follows:

$$\sigma_{RT} \simeq \frac{\sigma_P}{\mu_P^2} \qquad (Eq.2)$$

This approximation holds under the assumption that the distribution of promptness values is relatively normal and that the standard deviation is small compared to the mean.

2.4.2. Balance responses

To determine the onset of postural responses following a pulse perturbation, we examined the timing of measured muscle responses. This outcome measure relies on the muscle contraction in the mGAS , which generates ankle plantarflexion torque, to maintain balance after perturbation. The onset of the EMG response was determined using the mGAS, as it provided the most consistent response to the perturbations. EMG signals were high-pass filtered with a 2nd order Butterworth (30 Hz cut-off), then full-wave rectified and finally low-pass filtered with a 2nd order Butterworth (100 Hz cut-off). To obtain signals from which the onset of postural responses could be reliably identified, single-trial EMG signals were low-pass filtered (2nd order Butterworth, 20 Hz cut-off). To further reduce noise in the signals, an average was taken from the trials belonging to the same perturbation. This average was calculated over 25 bootstrapped samples (with replacement), each comprising 80% of the trials, to match the number of samples used in the reaction time dataset. Onset timing was defined as the first point where the EMG signal exceeded 2 SDs of a 400 ms baseline period (measured prior to trial onset) for at least 40 ms (Campbell, Dakin, and M. G. Carpenter 2009; Leeuwis et al. 2024). Onset timings lower than 50 ms or greater than 500 ms were excluded from analysis as being too early or too late to be related to the stimulus.

2.4.3. Statistical analysis

To estimate the effect size of the perturbation amplitude on the response times of the conscious detection and the postural response, estimation statistics were performed (Calin-Jageman and Cumming 2019; Ho et al. 2019). The response times were analysed in terms of promptness of button presses for conscious detection and the EMG onset for postural responses . Response time outcomes per perturbation amplitude were compared against those of the highest perturbation amplitude, 16 deg/s^2 for pulse-only and 1.6 SD for noise-only. The paired difference by trial order was taken to form the sampling distribution. 1000 bootstrapped means were obtained, forming a new distribution. The effect size, also known as the mean difference, is the mean of this distribution. The 95% CI of the mean difference estimates the sampling variability. To provide an estimate of the sampling error, the margin of error (MoE) was calculated from the CIs by averaging the length of the two CI arms. Statistics are reported as “mean difference ([lower CI bound, upper CI bound], MoE)”. The effect of ankle torque noise on the conscious detection and postural responses was estimated from the response times (RTs and EMG onset times) measured in the combined condition. Effect size estimation and statistical tests were performed in the same manner as for the pulse- and noise-only conditions. The effect size was estimated for the 3 s lead time trials, representing the presence of noise, and assessed separately for the two pulse amplitudes. Response time outcomes per noise SD level were compared against the 0 SD noise trials.

3

Results

To assess how different perturbation amplitudes affect conscious reaction time and the timing of postural responses, the pulse-only and noise-only conditions were analysed. During the pulse-only condition, participants experienced anterior perturbations at four pulse amplitudes In the noise-only condition, participants were presented with increased ankle torque noise of five different amplitudes. Participants were tasked to press the button whenever they detected an external perturbation. For analysis, only the first button press after noise onset was used as RT for that trial (Fig 2A). The timing of postural responses was extracted from EMG of the mGas (Fig 2D).

The effect of ankle torque noise on conscious detection and postural responses to balance disturbances was analyzed from the combined condition. In this condition, participants were presented with ankle torque noise interleaved with torque pulses at different lead times (0 or 3 s used in analysis). Participants were tasked with detecting the pulsed perturbation and ignoring the noise perturbation. (Fig. 2C)

3.1. Response times to pulsed torque balance perturbations

During the pulse-only conditions, participants were presented with pulsed torque perturbations. Conscious button presses throughout all trials are presented in Figure 3 for participants 2 and 6. For P2, the button presses per pulse amplitude occurred in visually distinct groups and response variability increased with decreasing torque amplitude (Fig. 3A). Participant 6 had was less variable in their responses (tight clusters) but had a higher detection threshold as they did not react to the 2 deg/s^2 pulses (black horizontal lines aligned with pulse onset Fig. 3B). In both, participant 2 and 6, as well as in the pooled data (Fig. 3C) it is apparent that RT decreased with increasing torque amplitude while response variability increased with decreasing amplitude. Additionally, detection probability rapidly increased with increasing torque amplitude (black horizontal lines at pulse onset in Fig. 3).

To assess the normality of the RT data and identify outliers, reciprobit plots were created (See Methods). The RTs from individual participants and pooled participants visually aligned with the fit made from the central quartiles of the data (Fig. 4A-C). Based on this, normality was verified for statistical analysis. The pooled reciprobit plot showed a single outlier with a low RT (RT = 126 ms); a cutoff of > 150 ms was used for data inclusion in further analysis. The reciprobit analysis confirmed the impression provided by the dotraster plots (Fig. 3). That is, mean RT increased with increasing torque amplitude while RT standard deviation decreased, i.e., participants became faster and less variable in their responses.

Figure 5A shows the pulse detection rate as a function of torque pulse amplitude for all participants (thin colored lines) and the average across participants (thick line). Participants were able to consistently detect the 4, 8, and 16 deg/s^2 pulses with detection rates exceeding 80% for all participants (0.92±0.06, 0.98±0.05, and 0.99±0.02). However, with the 2 deg/s^2 pulses, participants detected disturbances in only 51±26% of the trials, with one participant failing to detect any of the pulses. (Fig. 5A).

The RT of the conscious detection of pulsed balance disturbances decreases with increasing pulse

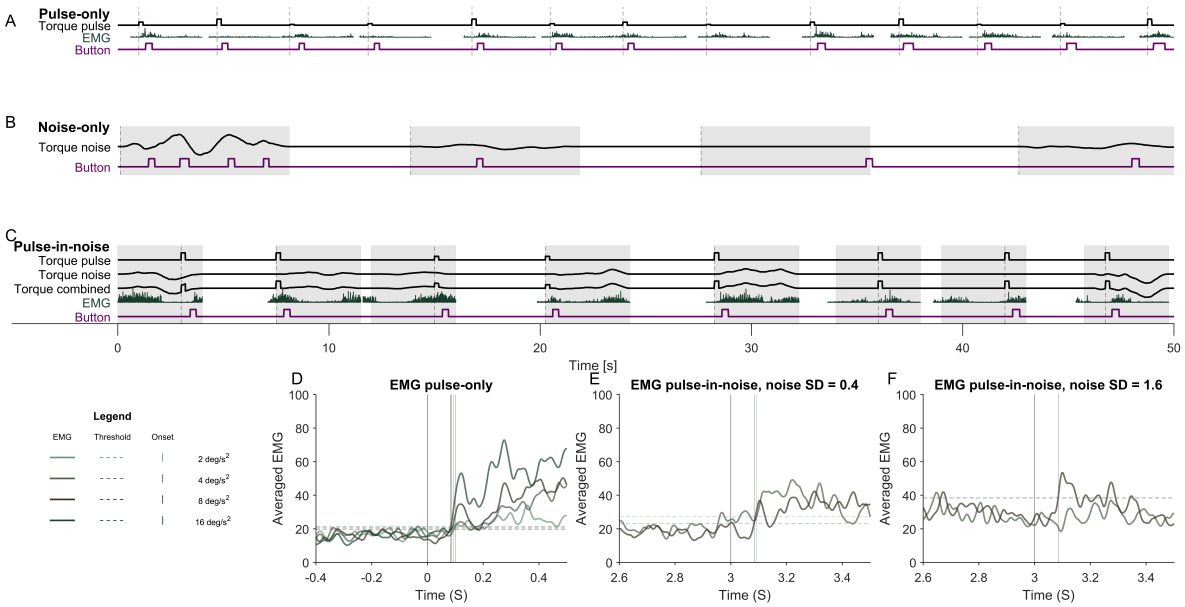

Figure 2. Sample data and perturbations and electromyography (EMG) processing example from a single participant (P2) (**A**) Time series of perturbation (Black), EMG (Green), and button presses (Purple) for pulse-only condition. In the pulse-only experiment, the perturbation torque signal consisted of 200 ms square pulses of 4 amplitudes. The dashed black line marks the onset of the perturbation. Participants were instructed to press the button when they detected a perturbation. The muscle activity rises before the button presses and is also present when perturbations are undetected. (**B**) Time series of perturbation (Black) and button presses (Purple) for noise-only condition. For the noise-only experiment, the perturbation signal consisted of 8 s periods of ankle torque noise (Gray shaded), or an 8-second period without perturbation. Participants were instructed to press the button whenever they detected a disruption to their balance control. The characteristics of the torque noise were derived from each participant's balancing torque signal in a baseline trial prior to completing the reaction time tasks (see Methods). Button presses occur more frequently in the strongest noise SD (Noise period 1), but even occur when noise is presented (Noise period 3). (**C**) Time series of perturbations (Black), EMG (Green) and button presses (Purple) for combined condition. In the combined experiment, the perturbation signals were added together, resulting in a combined signal. This consisted of 4 s noise periods (gray shaded) with 200 ms pulses starting at 0, 1, 2, or 3 s into the noise period (only 0 and 3 were included in the analysis). The dashed black line marks the onset of the pulse perturbation. In this condition, participants were tasked with pressing the button only when they detected the pulsed perturbations. Reaction times were extracted as the time between the onset of the perturbation and the button press. (**D**) Averaged EMG (Green) traces as resulting from the bootstrap averaging of single trial EMG signals for the pulse-only condition. Pulse onset at black line, t=0 s. Extracted onset times are depicted in blue. The strength of muscle activation decreases with increasing perturbation amplitude. (**E**) Averaged EMG (Green) traces as resulting from the bootstrap averaging of single trial EMG signals for the combined condition with 0.4 SD noise. Pulse onset at black line, t=3 s. Extracted onset times are depicted in blue. (**F**) Averaged EMG (Green) traces as resulting from the bootstrap averaging of single trial EMG signals for the pulse-only condition with 1.6 SD noise. Pulse onset at black line, t=3 s. Extracted onset times are depicted in blue. No onset was detected by the algorithm for the averaged EMG trace of the 4 deg/s^2 pulses.

amplitude (Fig. 5B purple). To quantify the influence of perturbation amplitude, estimation statistics were performed, comparing RTs per pulse amplitude to the RT of 16 deg/s^2 pulses. RT with lower pulse amplitudes differed significantly from the reference (Fig. 5C). With 2, 4, and 8 deg/s^2 resulting in a mean difference of 219 ([185, 263], 38) ms, 75 ([66, 85], 9) ms, and 22 ([17, 28], 5) ms. The perturbation pulses at all amplitudes evoked robust postural responses as seen in the recorded muscle activity (Fig. 2A). From these recordings, onset timings were extracted as an estimate of the response time of the automatic postural control. While EMG latencies were much faster (< 200 ms) than button-press reaction times (> 200 ms), EMG response time decreased with increasing pulse amplitudes (Fig. 5B green), like the conscious-detection reaction times. The estimated effect sizes of pulse amplitude on postural response time, while smaller compared to the conscious-detection reaction times, showed significant differences between the EMG onset timings in response to the highest pulse amplitude and the lower amplitudes (Fig. 5C). 2, 4 and 8 deg/s^2 pulses resulted in a mean difference of 95 ([86,103], 9) ms, 49 ([43,56], 7) ms, and 13 ([10,16], 3) ms. respectively.

Taken together, both conscious detection and postural responses to pulsed balance disturbances became faster with increasing torque pulse amplitude, indicative of similar underlying signal-detection processes.

3.2. Response times to increased ankle torque noise balance perturbations

In the noise-only condition, periods of increased ankle torque noise were presented to participants. The dotraster plots in Figure 3D-F show the raw button-press data for participants 2 (Fig. 3D) and 8 (Fig. 3E) and pooled across all participants (Fig. 3F). Compared to the pulse-only responses (Fig. 3A-C), participants responded much more often with more variable responses even in the control condition with a SD of zero (Fig. 3E-F). Nevertheless, clear and consistent responses occurred around 2 s, i.e. after the 1-second onset ramp. Some participants (Fig. 3E,F) had the tendency to respond during the 1-second onset ramp. These responses may not be stimulus related.

To determine whether the early presses visible in the dotraster plot were early responses not due to the stimulus, the reciprobit plots were created (Fig. 4D-F). For participant 2 (Fig. 4D), a single outlying data point in the SD = 0.4 condition can be seen that clearly deviated from the rest of the distribution. In contrast, the reciprobit plot of participant 8 shows a large number of early responses across all conditions that deviate from the fits of the central distribution (Fig. 4E), consistent with the high number of false detections in the 0 SD noise trials (Fig. 3E). The majority of early responses in the pooled distribution (Fig. 3F) were contributed by participant 8. Based on the pooled reciprobit, a cut-off of > 500 ms was decided for data inclusion in further analysis, removing 30 trials (3%).

RTs for the higher (1.2 and 1.6 SD) noise SD levels follow their respective fits well, but not very well for the lowest noise setting (0.4 SD). It is also clear from the pooled reciprobit plot (Fig. 3F) that RTs for the two lowest noise SD level (0.4 and 0, i.e. no perturbation) were not normally distributed, indicating that the underlying processes do not reflect simple signal detection models. This reflects the task difficulty and suggests the influence of more cognitive processes in the reaction to torque noise perturbations. Despite the indication of a non-normal 0.4 SD distribution, data analysis was performed under the assumption of normality for all noise SD levels.

Detection of balance disturbances by ankle torque noise increased with noise SD (0.4 SD : 0.73 ± 0.17, 0.8 SD: 0.90 ± 0.09, 1.2 SD: 0.92 ± 0.08, 1.6 SD: 0.94 ± 0.7)(Fig. 5D). At 0 SD noise, false detection occurred in 34 ± 27% of trails, with one participant pressing the button in 96% of trials.

RTs of detection of ankle torque noise decreases as noise SD increases (Fig. 5E). To quantify the influence of ankle torque noise amplitude on the RTs of conscious detection, estimation statistics were performed, comparing RTs per noise SD to the RT of 1.6 SD noise periods. All noise SD amplitudes show a significant difference in RT (Fig. 5C). The bootstrapped mean differences for 0.4, 0.8, and 1.2 SD are 1038 ([641,1527], 393) ms, 349 ([187,544], 179) ms, and 163 ([36,307], 135) ms. The higher mean RTs compared to even the lowest amplitude pulse stimuli suggest that the task of detecting the noise is more difficult for participants compared to the pulse perturbation.

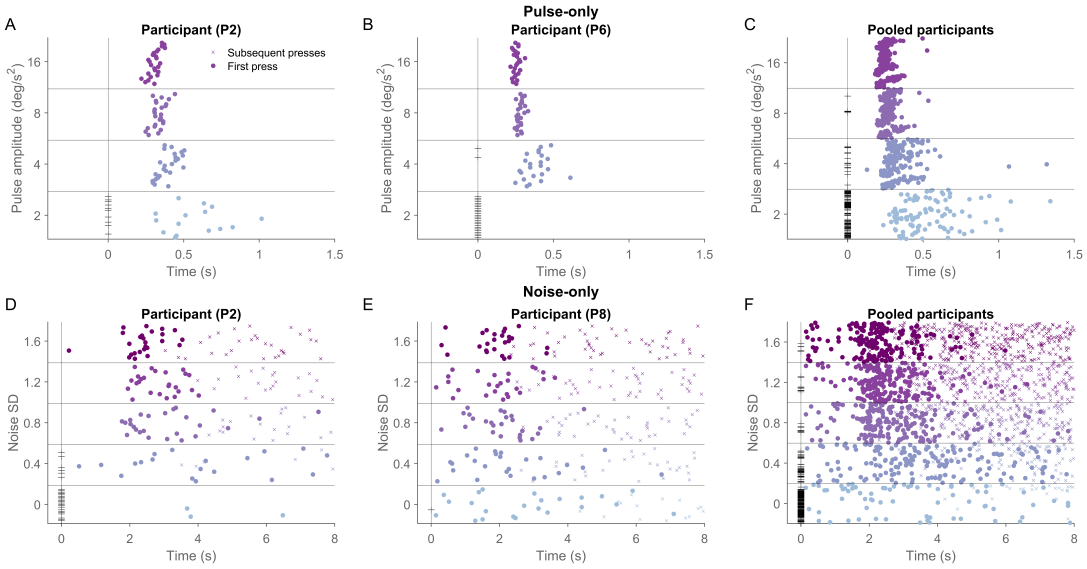

Figure 3. Raw data from pulse-only and noise-only experiments in dotraster plots. Trials are plotted stacked per condition. The onset of the perturbation occurred at t=0. The first button press (marked by filled dot, ●) was taken as reaction time (RT). Subsequent presses (marked by diagonal cross, ×) after the first were not included in the statistical analysis. Trials without a button press in the window are marked with a + at t=0. (**A**) Participant P2 showed increasing variance in RT with decreasing pulse amplitude, and more missed pulses for lower amplitudes. RTs slow with decreasing pulse amplitude. (**B**) Participant P6 had no detections of 2deg/s^2 pulses. This participant also showed a sudden increase in RT variance between 8 and 4 deg/s^2. (**C**) Pooled dotraster of all data from all participants. An increase in variance and mean of RT is observed with decreasing pulse amplitude. (**D**) Participant P2 showed occasional presses in 0 standard deviation (SD) noise (no perturbation) condition. Later RTs are more common in lower noise SD, and consecutive presses are more common in higher noise levels. RTs start occurring systematically from around 1.5 seconds. (**E**) Participant P8 pressed the button frequently throughout the experiment, as indicated by the large number of button presses in the 0 SD condition and consecutive presses at higher noise levels. This resulted in less dense clusters of RTs, as many early presses (RT<500 ms) were present. (**F**) Pooled dotraster of all data from all participants. Clusters of RTs form after 1.5 s when noise is presented, no cluster exists for the 0 SD condition.

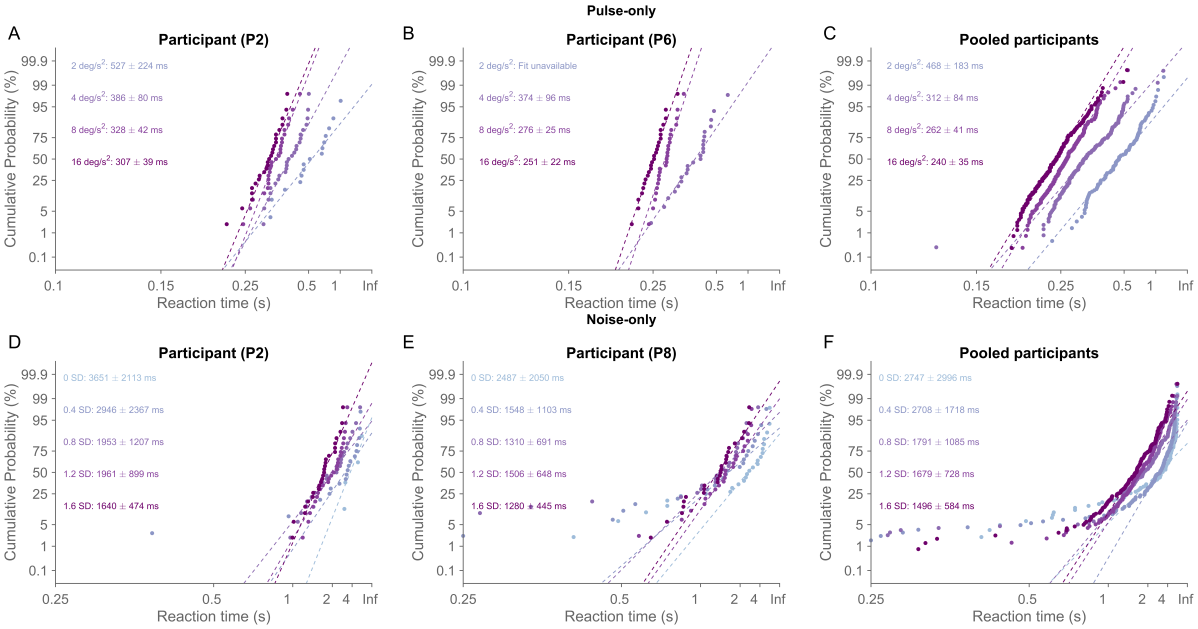

Figure 4. Raw data from pulse-only and noise-only experiments in reciprobit plots. Reciprobit plots present cumulative probability plotted against promptness. Promptness is the reciprocal of reaction time, and x-axis and labels have been converted to reaction time for legibility. A linear fit (dashed line) is performed on the inner quadrants of the distribution. Mean and standard deviation presented are based on the fit for the corresponding condition and converted from promptness to reaction time. (**A**) Participant P2 showed that the linear fit aligns with the data, indicating normal distribution of RTs. The slope of the fit decreases with pulse amplitude, reflecting the increase in variance within the conditions. (**B**) Data from participant P6 consists of tight distributions aligning with the fit for the highest two amplitudes, with a considerable increase in standard deviation at 4deg/s^2. Since no RTs were available for 2deg/s^2 no fit could be made. (**C**) Pooled data aligned well with the fits for each condition, indicating normal distribution for the pooled dataset and the absence of extreme outlier participants. A single outlying datapoint is visible at 128 ms, lying distant from both the distribution and the fit. Based on this, the exclusion criteria was set at RT < 150 ms (**D**) Participant P2 showed less clean alignment with the fit than in the pulse-only experiment. Overlapping distributions and fits indicate a smaller relative effect size. An outlying datapoint can be seen at 401 ms. (**E**) Participant P8 pressed the button frequently throughout the experiment. Multiple outlying datapoints can be seen plotted distant from their corresponding distribution and fit. Due to the large number of distant datapoints, the fit of 0.4 and 0.8 SD noise is pulled towards these early responses, resulting in a greater standard deviation. (**F**) Pooled data for all participants. A considerable number of early responses lie distant from their respective distributions and fit. Based on this, exclusion criteria was set at RT < 500ms. Apart from outliers, data for the higher two noise SD levels follow the fit, suggesting normal distributions. However, 0.4 and 0.8 SD noise form curved distributions, indicating that other processing is affecting the generation of reaction times, resulting in skewed distributions.

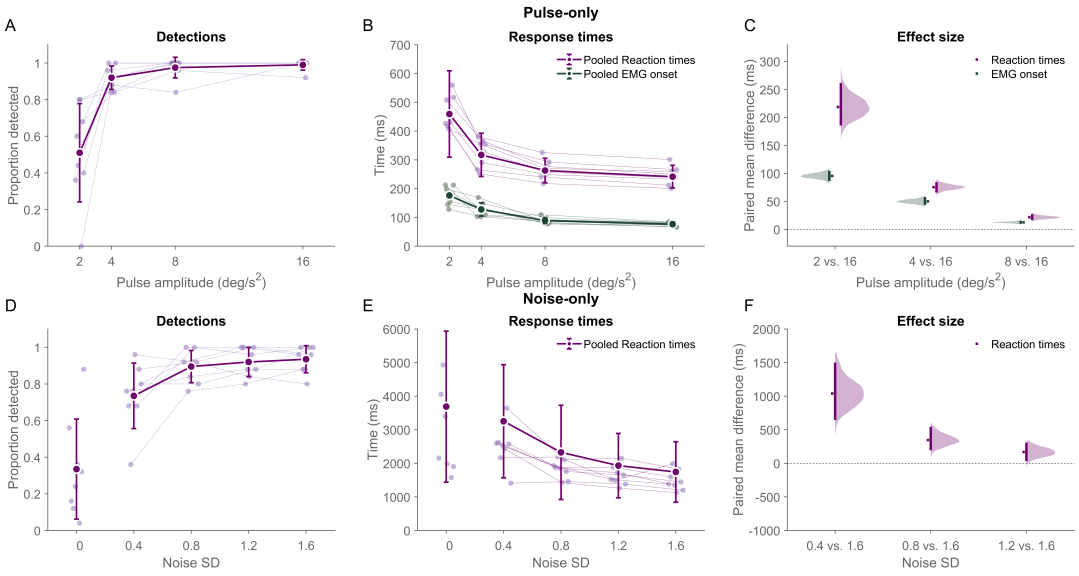

Figure 5. Detection proportions and response times for pooled data from pulse-only and noise-only experiments. Means and standard deviation (SD) of RTs are extracted from reciprobit fits on promptness and converted back to RT (**A**) Detection proportions for pulse amplitudes presented as group mean and SD; transparent markers indicate participant means. (**B**) RTs (Purple) and bootstrapped EMG onset times (Green) for increasing pulse amplitudes. Opaque markers represent group mean and SD, and transparent markers individual mean for RT and individual bootstrapped mean for EMG onset time. (**C**) Estimated effect size of RT (Purple, right-facing) and EMG onset time (Green, left-facing) comparing pulse amplitudes to 16deg/s^2. The shaded area represents the distribution of bootstrapped means with the 95% Confidence Interval (CI) as the line and mean at the marker. (**D**) Detection proportions for pulse amplitudes are presented as group mean and SD; transparent markers indicate participant means. 0 SD noise condition represents false detections under no perturbation condition and is therefore disconnected from conditions containing perturbation. (**E**) RTs (Purple) for increasing noise SD levels. Opaque markers represent group mean and SD, and transparent markers represent individual mean. 0 SD noise condition represents response times within a period without perturbation, and is therefore disconnected from perturbation conditions. (**F**) The estimated effect sizes of RT (Purple) comparing pulse amplitudes to 1.6 SD. The shaded area represents the distribution of bootstrapped means with the 95% Confidence interval, and the distribution mean as the black line and coloured marker, respectively.

3.3. Effect of increased ankle torque noise on balance perturbation response times

To study how increased noise in the balance control loop affects the detection of and postural responses to balance disturbances, participants were presented with simultaneous ankle torque noise and torque pulses in the combined condition. RTs to pulse perturbations even in the presence of noise were normally distributed for both the 0 and 3 s noise lead times, as illustrated in the pooled reciprobit plots, for which the majority of the data aligned with their linear fits (Fig. 6). The same outlier threshold of 150 m established from the pulse-only experiment was applied, resulting in the removal of only 5 data points from the pooled responses.

The pooled recibrobit of the 0 s lead time trials (Fig. 6A) shows that the RTs for 8 deg/s^2 pulses are faster than those for 4 deg/s^2, consistent with the findings from the pulse-only condition. Similarly, the standard deviation is lower for the 8 deg/s^2 pulses. The noise SD level does not have a noticeable influence on the mean of SD of the RT. Comparing this to Figure 6B, the 8 deg/s^2 pulse are still detected faster and with lower variability. However, it now shows a clear influence of noise level on the RTs, as the distributions lie further apart for each other. This is especially noticeable for the 4 deg/s^2 pulses.

The influence of noise on detections can also be seen from the detection rates depicted in Figure 7A. Almost all of the 8 deg/s^2 pulses (Fig. 7A red) were detected across all noise levels and delay times, with only the highest noise level bringing the proportion of detected pulses down to 0.86 ± 0.11. Pulses of 4 deg/s^2 (Fig. 7A blue) were detected less in the 0 s no-noise condition compared to the higher pulse amplitude, but were still consistently detected, with detection rates exceeding 80% for all noise SD levels (0 SD: 0.92 ± 0.11, 0.4 SD: 0.93 ± 0.07, 0.8 SD: 0.89 ± 0.11, 1.2 SD: 0.91 ± 0.09, 1.6 SD: 0.93 ± 0.05). When the pulse was presented within the noise, the proportion of detected pulses decreased

with increasing noise SD. Noise SDs of 0, 0.4, 0.8, 1.2, and 1.6 resulted in detection proportions of 0.92 ± 0.09, 0.87 ± 0.13, 0.74 ± 0.15, 0.63 ± 0.19, and 0.52 ± 0.22.

The effect of ankle torque noise on the response times of conscious detections and automatic postural responses is stronger on the lower pulse amplitude pulses of 4 deg/s^2 (Fig. 7B blue). In the 0 s lead time trials, the RTs are independent of the SD noise level. However, when pulses are presented 3 s after the noise has started, the RTs of conscious detections increase with noise SD level (0 SD: 385 ± 122 ms, 0.4 SD: 405 ± 150 ms, 0.8 SD: 419 ± 205 ms, 1.2 SD: 494 ± 237 ms, 1.6 SD: 487 ± 226 ms). Effect size estimation comparing RTs in presented noise levels against 0 SD revealed an increasing significant mean difference depending on noise level for 0.8 SD noise and greater (0.4 SD: 19 ([-10, 59], 40) ms, 0.8 SD: 50 ([6, 95], 45) ms, 1.2 SD: 130 ([73, 199], 63) ms, 1.6 SD, 149 ([82, 227], 73) ms) (Fig. 7D blue). This systematic influence of increasing noise SD on conscious RTs is also present for the detection of 8 deg/s^2 pulses (Fig. 7C red). Again, in the 0 s lead time trials, RT is not dependent on the noise SD, but RTs increase with noise SD in the 3 s lead time trials (0 SD: 311 ± 70ms, 0.4 SD: 311 ± 70ms, 0.8 SD: 321 ± 80 ms, 1.2 SD: 336 ± 105ms, 1.6 SD: 345 ± 117 ms). The effect sizes are smaller than on the detections of 4 deg/s^2 pulses, but still increase with noise level after noise reached 0.8 SD (0.4 SD, 3 ([-9, 15], 12) ms, 0.8 SD: 14 ([1, 27], 13) ms, 1.2 SD: 32 ([17, 50], 17) ms, 1.6 SD, 47 ([28, 65], 19) ms) (Fig. 7E red).

While the RTs increase in higher noise SD trials, the onset timing of postural responses does not follow this pattern. In both the 4 deg/s^2 and the 8 deg/s^2 trials, EMG onset times did not increase with increased noise SD (Fig. 7B-C green). For the smaller pulse amplitude, the mean EMG onset time for the 0 s lead time was faster than in the 3 s lead time trials (0s: 132 ± 58 ms, 3s: 144 ± 62 ms). However, no systematic pattern dependent on noise SD was present 0 SD: 132 ± 35 ms, 0.4 SD: 127 ± 38 ms, 0.8 SD: 150 ± 19 ms, 1.2 SD: 131 ± 18 ms, 1.6 SD: 170 ± 37 ms. The estimated effect sizes show a significantly higher onset time in response to 0.8 SD noise when compared to in 0 SD noise trials (Fig. 7D green). No significant effect was found for the 0.4 and 1.2 noise SD trials (0.4 SD: -10 ([-22, 3], 10) ms, 1.2 SD: 8 ([-8, 20], 14) ms). A significant effect was present for both the 0.8 and 1.6 SD noise levels (0.8 SD: -21 ([6, 33], 14) ms, 1.6 SD: -24 ([4, 43], 20) ms). Similarly, for the 8 deg/s^2 pulses, the timing of postural responses did not increase with increasing ankle torque noise (0 SD: 92 ± 6 ms, 0.4 SD: 84 ± 9 ms, 0.8 SD: 108 ± 27 ms, 1.2 SD: 90 ± 9 ms, 1.6 SD: 69 ± 24 ms)(Fig. 7C). When compared to the 0 SD noise trials, a significant decrease in EMG onset time was found in the 0.4 SD noise trials and increases in the 0.8 and 1.6 SD trials (0.4 SD: -7 ([-10, -4], 3) ms, 0.8 SD: -21 ([14, 29], 8) ms, 1.2 SD: -1 ([-4, 3], 4) ms, 1.6 SD: 9 ([4, 16], 6) ms) (Fig. 7E green). No effect was observed for the 1.2 SD noise trials.

Taken together, only the conscious detection of balance disturbances is affected by the signal-to-noise ratio of the target signal, while the onset of postural responses is unaffected. This indicates these processes have separate pathways for processing sensory information.

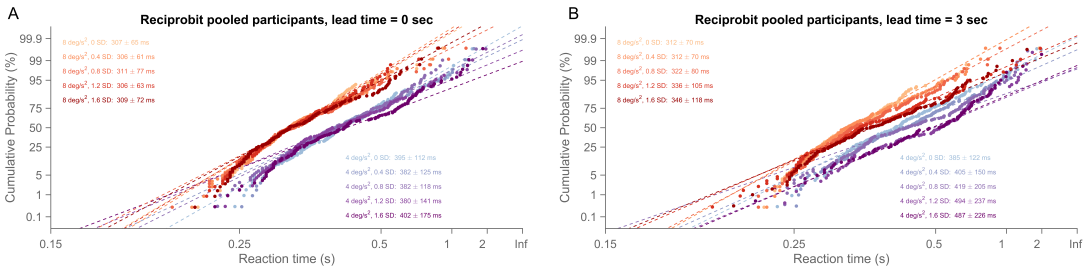

Figure 6. Raw data from the combined experiment in reciprobit plots. Reciprobit plots present cumulative probability plotted against promptness. Promptness is the reciprocal of reaction time (RT), and the x-axis and labels have been converted to RT for legibility. A linear fit (dashed line) is performed on the inner quadrants of the distribution. The mean and standard deviation presented are based on the fit for the corresponding condition and converted from promptness to reaction time. Conditions are noted as [pulse amplitude, noise standard deviation (SD)]. (**A**) Reciprobit for pooled RT data of pulses presented at 0s-lead time compared to noise onset. Distributions for 4 and 8 deg/s^2 pulses are parallel, indicating a difference in RT between conditions, while within pulse conditions distributions are overlapping, suggesting no difference dependent on noise SD level. The data visually aligns with the fit for most conditions; however, for 4 deg/s^2 pulses presented with 1.2 and 1.6 SD noise levels, the data deviates more from the linear fit, suggesting non-normally distributed data. (**B**) Reciprobit for pooled RT data of pulses presented at 3s-lead time compared to noise onset. Distributions for 4 and 8 deg/s^2 pulses are parallel, indicating a difference in RT between conditions. Within pulse conditions, distributions are also parallel, suggesting an effect on RT dependent on the noise SD level. The data visually aligns with the fit for most conditions, suggesting normal distribution of promptness data.

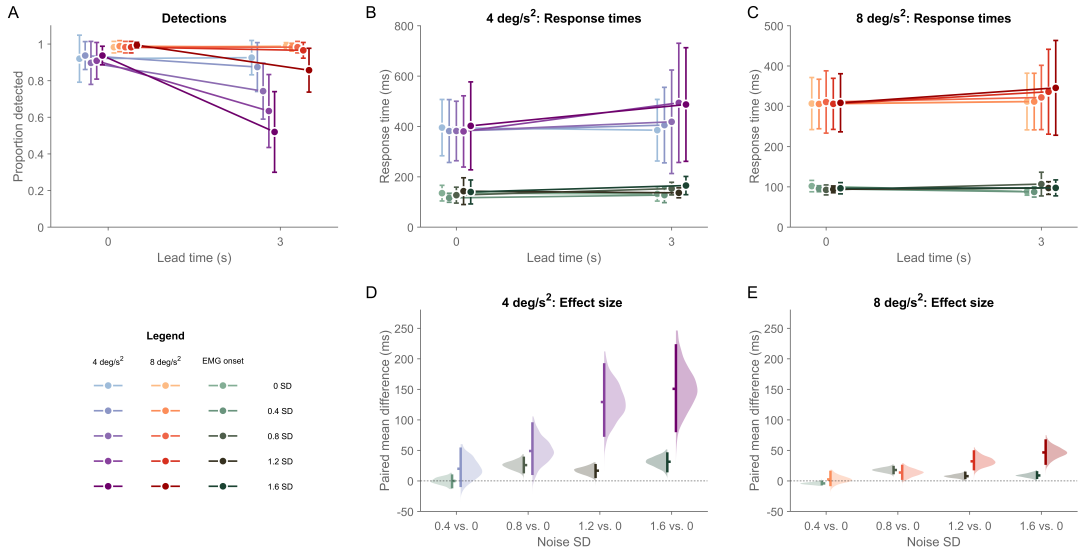

Figure 7. Detection proportions, response times, and estimated effect size for pooled reaction time (RT) data from the combined experiment. Means and standard deviation (SD) of RTs are extracted from reciprobit fits on promptness and converted back to RT. Conditions are noted as [pulse amplitude, noise standard deviation (SD)]. (**A**) Detection proportion per condition presented as mean ± SD. Detection proportions are close together for both pulse amplitudes at 0s-lead time (mean [range of means]), 4 deg/s^2: 0.91 [0.89-0.93] and 8 deg/s^2: 0.98 [0.98-0.99]. The detection proportion decreases along with the noise SD level for 4 deg/s^2 pulses at 3s-lead time to (noise SD: mean ± SD) 0 SD: 0.92 ± 0.09, 0.4 SD: 0.87 ± 0.13, 0.8 SD: 0.74 ± 0.15, 1.2 SD: 0.63 ± 0.19 and 1.6 SD: 0.52 ± 0.22. (**B**) RT (Purple) and EMG (Green) onset times to 4 deg/s^2 pulses. (**C**) RT (Orange) and EMG (Green) onset times to 8 deg/s^2 pulses. (**D**) Estimated effect size of noise SD on response times for 4 deg/s^2 pulses. The shaded area represents the distribution of bootstrapped means with the 95% Confidence Interval (CI) as the line and mean at the marker. The distributions of the effect size on RTs are purple and right-facing, and on EMG onsets, green and left-facing. (**E**) Estimated effect size of noise SD on response times for 8 deg/s^2 pulses. The shaded area represents the distribution of bootstrapped means with the 95% Confidence Interval (CI) as the line and mean at the marker. The distributions of the effect size on RTs are orange and right-facing, and on EMG onsets, green and left-facing.

4

Discussion

In this study, the mechanisms underlying conscious detection and automatic postural responses to balance disturbances were investigated by their sensitivity to perturbation amplitude and signal-to-noise ratio. The pulse-only condition revealed that increasing the amplitude of torque pulse perturbations results in significantly faster response times, both for RTs representing conscious detection and the EMG measured onset times of the postural responses. A similar result was observed in the noise-only condition, where participants responded faster to greater noise amplitudes. These results indicate that pathways leading to conscious detection and postural responses have similar decision-making processes. The pulse-in-noise condition revealed that conscious RTs of pulsed balance disturbances were significantly slower when presented with greater ankle torque noise. However, the onsets of automatic postural responses did not show the same systematic effect dependent on noise level. This reveals a difference in the underlying pathways used to initiate conscious detections and postural responses. Collectively, these results show that the pathways for balance information in the nervous system are geared towards different functional purposes. The conscious detection of balance disturbances considers both the strength of the disturbance and the signal-to-noise ratio. While for automatic postural control, only the strength of the perturbation determines the response time.

4.1. Reaction times of the conscious detection of balance perturbations increase with perturbation amplitude

In the pulse-only condition, participants were presented with four amplitudes of pulsed torque perturbations. RTs to these stimuli increased when perturbation amplitudes decreased. This result is similar to that of (Richerson et al., 2004), where increasing the amplitude of support surface translations resulted in faster RTs. RT in response to the pulsed perturbations also shows a normal distribution when transformed to its reciprocal, promptness. These characteristics are commonly found in RT studies into sensory systems and have been described using the Linear Approach to Threshold with Ergodic Rate (LATER) model (Noorani & Carpenter, 2016). In a single unit of this model, detection of a stimulus occurs when the set decision threshold is reached. Presenting a stimulus makes the decision signal start increasing from its baseline state. This is modelled as a linear increase, where the rate of the increase is dependent on the stimulus amplitude. As the stimulus amplitude determines the rate and the threshold is independent of the of the stimulus amplitude, greater stimulus amplitudes result in the decision signal reaching its threshold faster. This characteristic is reflected in the response times to balance perturbations measured in the pulse-only and noise-only. In the LATER model, the rate of rise is modelled as having a Gaussian distribution within identical stimulus amplitudes. This results in the distribution of response times when the decision threshold is reached being skewed, and its reciprocal being normally distributed. RTs measured for pulsed balance perturbations reflect this behaviour as the promptness distributions are normally distributed. As the results from the pulse-only condition follow the LATER model, this would suggest that the conscious detection of pulsed balance disturbances relies on a set threshold with a varying rate of rise of the decision signal to reach detection. Therefore, conscious detection of balance disturbances seems to be a simple process that is identical to detec-

tion in other modalities, in that reaction time is inversely related to stimulus strength (Mansfield 1973; Posner 1980; Prinzmetal, McCool, and Park 2005).

The noise-only condition did not follow the LATER model's prediction of normally distributed promptness data. This indicates that more complex processes may be required for the detection of ankle torque noise. One possibility is that two units of the LATER model are competing, with the first to reach their threshold resulting in conscious detection (Noorani and Carpenter, 2016). In the case of two competing units, the promptness distribution visible in the reciprobit plot would consist of two linear components. The early responses seen in the dotraster and reciprobits plots for the noise-only condition may be the results of a two unit LATER model type of processing, which would explain why the overall promptness distribution does not follow a single linear fit. However, it should be considered that the early presses resulted from variation in the perturbation itself. As the perturbation is generated from white noise signals, trails with high amplitude peaks early on in the noise perturbation may occur and result in early presses. The variation in signal amplitude across trials of the same noise SD could also contribute to greater variance in the rate of rise of the decision signal, making it more difficult to determine the existence of a competing LATER unit. The reaction times to the noise are also considerably longer than the most common applications of simple LATER models.

While considerably slower than the RTs to pulse perturbations, the RTs are almost twice as fast to equivalent noise stimuli presented in Messink et al. (2025). This difference in RTs may be due to the difference in task. In the current study, participants were asked to respond whenever a disturbance was detected, while in Messink et al. (2025), participants were instructed to indicate when they percieved the stimulus to be present until they were sure it was turned off. The lowest provided noise SD level in this study is only just below the 70% threshold identified by Mensink et al. (2025) of 0.43 SD and resulted in a comparable perception proportion of 0.74±0.17, indicating similar perceptual detection difficulty.

4.2. Muscle activation onset timing is dependent on perturbation amplitude

The muscle activation onset timings extracted from the EMG signal of the gastrocnemius muscle in response to pulsed torque perturbations increased significantly when perturbation amplitudes were lower. This relationship between response time and stimulus amplitude suggests that the balance controller operates according to the LATER model. However, since individual trial EMG signals were not analyzed, the distribution of the per-trial response times could not be inspected. Therefore, the characteristic of response time forming a normal distribution when converted to its reciprocal was not evaluated. While amplitude-dependent response times do still suggest the postural responses are initiated based on a decision-making process similar to that of the LATER model, the finding of amplitude-dependent response times has not been found in previous studies (Diener, Horak, and Nashner 1988; Horak, Diener, and Nashner 1989). This difference could stem from how onset timings are determined. Diener et al. (1988) and Horak et al. (1989) manually set the onset of the EMG response, whereas this study utilized a two-threshold automated detection algorithm. A preliminary investigation of the algorithm reveals that the shapes of the activation patterns (Fig. 2D) for different perturbation amplitudes may lead to an overestimation of response time. However, this effect does not explain the full estimated effect size. Additionally, visual inspection of the onset timings determined by the algorithm reveals no substantial differences from those manually placed. Taken together, these limitations do not explain the full effect size, suggesting that the timing of postural responses is inversely related to perturbation amplitude. This indicates that the automatic postural control follows the LATER model and thus maintains a set decision threshold for initiating postural responses.

4.3. Added motor noise influences the conscious sense of balance without affecting muscle activation timings

The combined condition revealed an increasing significant effect of ankle torque noise SD on the detection of pulsed balance perturbations. However, no systematic pattern of the effect of noise SD on postural response timings was found. This suggests that different underlying decision-making processes are used for detection.

The role of the signal-to-noise ratio in the decision-making process underlying conscious detection is revealed by the smaller effect size of noise SD on the RT for 8 deg/s^2 pulses compared to 4 deg/s^2 pulses. When there is more uncertainty in the decision-making process, it may be beneficial for the detection system to raise its decision threshold to avoid errors (Noorani and R. H. Carpenter 2016). The conscious detection process takes into account the increased uncertainty by increasing its decision threshold accordingly. A set increase in this threshold for a certain noise SD would result in a greater effect size for the smaller perturbations. They have a slower rate of rise and will therefore take longer to accumulate the same difference in evidence required by the new threshold than a perturbation with a higher rate of rise. The threshold modulation also explains the slower RT for pulses in the no-noise (0 s lead time) trials of the pulse-in-noise condition compared to RTs of similar pulse amplitudes in the pulse-only condition. While the noise is not constantly present throughout the combined conditions, the participants cannot predict the onset of the noise, providing additional uncertainty throughout the entire condition. Importantly, the automatic postural responses do not slow down based on the level of uncertainty, suggesting that the balance control system does not modulate its decision-thresholds based on the uncertainty of the context. Similarly, the EMG onsets in the no-noise trials of the combined condition are the same as those for equivalent pulse amplitudes in the pulse-only condition. These results indicate that the conscious detection of balance disturbances may modulate its decision threshold to avoid errors in detection. At the same time, automatic postural control does not alter its decision process in response to increased uncertainty.

These different mechanisms are required as both pathways fulfill different functions. The automatic postural control appears to detect the sudden disturbance of balance and initiate a corrective muscle response, regardless of the strength of the surrounding ankle torque noise. The purpose of the automatic postural control is to maintain standing balance, which requires responding to disturbances regardless of the type of perturbation or the surrounding context. However, the conscious detection process tries to analyse the sensory signals to discern the pulse from the surrounding noise. More processing is required for this purpose, but the conscious detection would have more information available, as the motor response of the automatic control occurs before the detection. While an ideal decision-making process for conscious detection would utilize information from automatic postural control to achieve the fastest reaction time, this information may not be available to conscious processing. Luu (2010) shows that the active force generated during standing is not fully consciously perceived because it originates from a sub-cortical system to which the cortex may not gain perceptual access. This results in the conscious detection forming its own neural representation of the state of balance while relying on the same sensory information as the automatic postural control. The difference in response times could also originate from different weightings of the sensory information between the conscious detection and automatic control. Previous studies have investigated the weight and gains of the sensory systems involved in standing balance (Peterka 2002; Forbes et al. 2016). However, these studies have thus far only focused on the control of balance and not on the conscious detection of disturbances. A direct comparison between these two systems could reveal further evidence of the separate pathways for postural control and conscious detection of disturbances maintained by the nervous system.

4.4. Conclusion

This study demonstrated how the nervous system consciously detects and effectively corrects for imposed balance perturbations using two separate pathways of information processing. Both systems, individually, act according to sensory evidence accumulation models. The conscious sense of balance responds significantly faster to higher-amplitude perturbations, both to broadband pulsed torque perturbations and motor noise within participants' dynamic range. Postural responses, which were evoked over a time period reflecting subcortical contributions to balance, also started significantly faster in response to stronger disturbances. Investigating the role motor noise plays in the detection of balance disturbances revealed a pattern in which noise level systematically affected conscious RTs without affecting the onset of muscle activation in response to balance perturbations. Together, these findings suggest that for the conscious detection of balance, sensory evidence of disturbances is processed separately from the subcortical systems of the balance controller. While both processes rely on evidence accumulation mechanisms, only the conscious detection of disturbances is dependent on the signal-to-noise ratio of the disturbance.

References

Calin-Jageman, R. J. and G. Cumming (2019). “Estimation for Better Inference in Neuroscience”. In: *eneuro* 6.4, ENEURO.0205–19.2019.

Campbell, A. D., C. J. Dakin, and M. G. Carpenter (2009). “Postural responses explored through classical conditioning”. In: *Neuroscience* 164.3, pp. 986–97.

Carpenter, R. H. S. and M. L. L. Williams (1995). “Neural computation of log likelihood in control of saccadic eye movements”. In: *Nature* 377.6544, pp. 59–62.

Delorme, A. and S. Makeig (2004). “EEGLAB: an open source toolbox for analysis of single-trial EEG dynamics including independent component analysis”. In: *J Neurosci Methods* 134.1, pp. 9–21.

Diener, H. C., F. B. Horak, and L. M. Nashner (1988). “Influence of stimulus parameters on human postural responses”. In: *J Neurophysiol* 59.6, pp. 1888–1905.

Donders, F. C. (1969). “On the speed of mental processes”. In: *Acta Psychologica* 30, pp. 412–431.

Forbes, P. A. et al. (2016). “Transformation of Vestibular Signals for the Control of Standing in Humans”. In: *J Neurosci* 36.45, pp. 11510–11520.

Gurfinkel, V. S. et al. (1988). “Body Scheme in the Control of Postural Activity”. In: *Stance and Motion: Facts and Concepts*. Ed. by V. S. Gurfinkel et al. Springer US, pp. 185–193.

Ho, J. et al. (2019). “Moving beyond P values: data analysis with estimation graphics”. In: *Nat Methods* 16.7, pp. 565–566.

Horak, F. B., H. C. Diener, and L. M. Nashner (1989). “Influence of central set on human postural responses”. In: *J Neurophysiol* 62.4, pp. 841–853.

Jacobs, J. V. and F. B. Horak (2007). “Cortical control of postural responses”. In: *J Neural Transm* 114.10, pp. 1339–1348.

Jensen, J. L. W. V. (1906). “Sur les fonctions convexes et les inégalités entre les valeurs moyennes”. In: *Acta Mathematica* 30, pp. 175–193.

Kandel, E. R. et al. (2021). “Principles of Neural Science”. In: *Principles of Neural Science, 6e*. McGraw Hill.

Kiemel, T., K. S. Oie, and J. J. Jeka (2002). “Multisensory fusion and the stochastic structure of postural sway”. In: *Biol Cybern* 87.4, pp. 262–277.

Leeuwis, M. et al. (2024). “Different mechanisms of contextual inference govern associatively learned and sensory-evoked postural responses”. In: *Proc Natl Acad Sci USA* 121.32, e2404909121.

Luu, B. (2010). “Perception, perfusion and posture”. PhD thesis. UNSW Sydney.

Luu, B. L. et al. (2012). “Human standing is modified by an unconscious integration of congruent sensory and motor signals”. In: *J Physiol* 590.22, pp. 5783–5794.

Mansfield, R. J. (1973). “Latency functions in human vision”. In: *Vision Res* 13.12, pp. 2219–2234.

Massion, J. (1994). “Postural control system”. In: *Curr Opin Neurobiol* 4.6, pp. 877–887.

Mensink, L. H. et al. (2025). “The sense and control of standing balance in the presence of motor noise”. In: *(in preparation)*.

Noorani, I. and R. H. Carpenter (2016). “The LATER model of reaction time and decision”. In: *Neurosci Biobehav Rev* 64, pp. 229–251.

Palmer, J., A. C. Huk, and M. N. Shadlen (2005). “The effect of stimulus strength on the speed and accuracy of a perceptual decision”. In: *J Vis* 5.5, pp. 376–404.

Perotto, A. and E. F. Delagi (2005). *Anatomical Guide for the Electromyographer: The Limbs and Trunk*. Charles C Thomas.

Peterka, R. J. (2002). “Sensorimotor integration in human postural control”. In: *J Neurophysiol* 88.3, pp. 1097–1118.

Posner, M. I. (1980). “Orienting of attention”. In: *Q J Exp Psychol* 32.1, pp. 3–25.

Prinzmetal, W., C. McCool, and S. Park (2005). “Attention: reaction time and accuracy reveal different mechanisms”. In: *J Exp Psychol Gen* 134.1, pp. 73–92.

Qiao, C. Z. et al. (2023). “Multidirectional Human-in-the-Loop Balance Robotic System”. In: *IEEE Robot Autom Lett* 8.7, pp. 3948–3955.

Rasman, B. G., J. S. Blouin, et al. (2024). “Learning to stand with sensorimotor delays generalizes across directions and from hand to leg effectors”. In: *Commun Biol* 7.1, p. 384.
Rasman, B. G., P. A. Forbes, et al. (2018). “Sensorimotor Manipulations of the Balance Control Loop–Beyond Imposed External Perturbations”. In: *Front Neurol* 9, p. 899.
Ratcliff, R. (1993). “Methods for dealing with reaction time outliers”. In: *Psychol Bull* 114.3, pp. 510–532.
Richerson, S. J. et al. (2004). “Factors affecting reaction times to short anterior postural disturbances”. In: *Med Eng Phys* 26.7, pp. 581–586.
Tisserand, R. et al. (2022). “Unperceived motor actions of the balance system interfere with the causal attribution of self-motion”. In: *PNAS Nexus* 1.4, pgac174.
Ulrich, R. and J. Miller (1994). “Effects of truncation on reaction time analysis”. In: *J Exp Psychol Gen* 123.1, pp. 34–80.
Veugen, L. C. E., A. J. van Opstal, and M. M. van Wanrooij (2022). “Reaction Time Sensitivity to Spectrotemporal Modulations of Sound”. In: *Trends Hear* 26, p. 23312165221127589.
Whelan, R. (2008). “Effective Analysis of Reaction Time Data”. In: *Psychol Rec* 58.3, pp. 475–482.
Wolpert, D. M., Z. Ghahramani, and M. I. Jordan (1995). “An internal model for sensorimotor integration”. In: *Science* 269.5232, pp. 1880–1882.